



Original article

Synergistic performance of a Gemini nano ionic liquid and sodium dodecyl sulfate surfactants at the crude oil–water interface

Javad Saien*, Asma Eghtenaie, Mona Kharazi*

Faculty of Chemistry and Petroleum Science, Bu–Ali Sina University, Hamedan 6517838695, Iran

ARTICLE INFO

Article history:

Received 20 May 2023

Accepted 4 October 2023

Available online 7 October 2023

Keywords:

Gemini surface active ionic liquid

SDS

Interfacial tension

Emulsification

Wettability

ABSTRACT

Gemini surface active ionic liquids (GSAILs) are known as effective and environmentally friendly materials. Conventional anionic surfactants like sodium dodecyl sulfate (SDS), on the other hand, can establish desired properties in solutions. This study reports investigation on the influence of the mixtures of an imidazolium cationic GSAIL, $[C_4im-C_6-C_4im][Br]_2$, and the SDS anionic surfactant on the interfacial tension (IFT), emulsification, and wettability alteration of the crude oil–water system. Results demonstrate amazing synergistic effects, resulting in 97.1 % more IFT reductions compared to what could be achieved with the linear contribution of surfactants. Under the GSAIL mole fraction of 0.4 and the mixture concentration of $0.25 \text{ mol}\cdot\text{dm}^{-3}$ in aqueous phase, a low IFT of $0.18 \text{ mN}\cdot\text{m}^{-1}$ was attained. This is attributed to the attractive interaction between the involved surfactants. Synergisms of 52.0 and 59.8 % were also achieved in emulsification and wettability alteration with the mixture of surfactants under the optimum GSAIL mole fraction of 0.4. The obtained data for the individual and the mixture of surfactants were analyzed based on, respectively, Frumkin adsorption isotherm and the “non-ideal interactions in binary mixtures” theory. Corresponding consistent parameters were determined and discussed.

© 2023 The Author(s). Published by Elsevier B.V. on behalf of King Saud University. This is an open access article under the CC BY-NC-ND license (<http://creativecommons.org/licenses/by-nc-nd/4.0/>).

1. Introduction

Demand for crude oil, as the major source of energy, is growing worldwide; but, unfortunately, primary and secondary recoveries produce only 20 to 40 % of crude oils in mature reservoirs (Tamayo-Mas et al., 2016). Accordingly, injection of surfactants to reduce crude oil–water interfacial tension (IFT), as well as forming stable emulsions, and altering the wettability of rocks has been identified as a promising technique in enhanced oil recovery (EOR) (Kharazi et al., 2022, Hui et al., 2020). The main challenges in this technique and when using conventional surfactants are their sensitivity to salinity and temperature, leading their activity to diminish under harsh reservoir conditions (Rosen and Kunjappu, 2012). In this regard, amphiphilic nature surface active ionic liquids (SAILs) have received much attention in recent years. They exhibit

remarkable desired properties such as minor vapor pressure, stability, recyclability and non-toxicity (Kharazi et al., 2022). Notably, from economical point of view, SAILs are rather expensive and low cost-effective compared to the conventional surfactants (Saien et al., 2022).

For successful EOR purposes, it has been emphasized that the IFT of crude oil–water system has to be diminished to low values (Bera and Belhaj, 2016). Thus, addition of just a SAIL could be non-efficient (Rosen and Kunjappu, 2012). It is while, the mixture of a SAIL and a conventional surfactant can create synergism and reduce the IFT to a much greater extent, which is important and cost-effective case for eliminating surfactant flooding problems in EOR. In this regard, Jia et al., (2017) demonstrated that the mixture of cationic and anionic surfactants can significantly affect the IFT of the system of water–model oil (toluene + n-decane). Also, recently, Xu et al. reported that the various single-chain SAIL/surfactant mixtures bring about much better interfacial properties for the crude oil–water system and higher oil recoveries would be feasible compared to the case of using individual surfactants (Xu et al., 2023).

Gemini surface active ionic liquids (GSAILs), have been recognized with high interface activity as well as environmentally friendly nature. The molecular structure of GSAILs are consisted of two hydrophobic chains and hydrophilic head groups, connect-

* Corresponding authors.

E-mail addresses: saien@basu.ac.ir (J. Saien), kharazi.mona@yahoo.com (M. Kharazi).

Peer review under responsibility of King Saud University.



Production and hosting by Elsevier

ing with a spacer chain (Nessim et al., 2018). Compared to single-chain SAILS, the high level amphiphilic nature of GSAILS gives favorable properties in interfacial activity, resistance against salinity and thermal effects (Kharazi and Saïen, 2022a, Ezzat et al., 2021). Compared to other GSAIL families such as pyridinium, morpholinium and pyrrolidinium; imidazolium GSAILS have exhibited higher interfacial activity (Kharazi et al., 2022, Hou et al., 2022). Adding to these, their nano-size structure, even in solutions, improves the interfacial and thermo-physical properties of GSAILS (Chen et al., 2018).

In this context and in continuation of our previous studies in upgrading the performance of the surfactants in EOR (Kharazi and Saïen, 2022b, Kharazi et al., 2021, Saïen and Asadabadi, 2011), present study investigates the effects of the mixture of a nano-size imidazolium-based cationic GSAIL namely [C₄im-C₆-C₄im][Br]₂ (four carbons alkyl chains and six carbons spacer group) and the well-known anionic surfactant sodium dodecyl sulfate (SDS). The IFT reduction, critical micelle concentration (CMC), emulsification and wettability alteration of a crude oil–water system are investigated with mixtures. Given the point that most researches on EOR are based on single chain SAILS; use of the GSAIL and its mixture is a new endeavor here. For a deeper investigation, the results are compared with the effects of individuals and also, theoretical parameters are determined using appropriate models. Effects of the surfactant mixture on the emulsification and wettability alteration are also investigated. This study seems comprehensive since close to real employed operating conditions.

2. Experimental section

2.1. The used materials

The anionic surfactant SDS (purity > 99 %) was purchased from Merck. The imidazolium-based cationic GSAIL consisting of four carbons in the alkyl chains and six methylene spacer group with bromine anions, namely [1, 1'-(Hexane-1, 6-diyl) bis (3-butyl-1H-imidazol-3-ium) bromide], abbreviated as [C₄im-C₆-C₄im][Br]₂ (Fig. 1), was prepared by a one-pot synthesis method (Kharazi et al., 2019) with high purity. For this aim, a mixture of 1-butylimidazole (12.4 g, 100 mmol) and 1,4-dibromobutane (10.8 g, 50 mmol) was refluxed in acetonitrile (100 mL) for three days. Afterward, the solvent was removed and the crude product was thoroughly washed with tetrahydrofuran (3 × 30 mL) to yield the desired target product. The purity and the nano-size structure of the GSAIL were confirmed by ¹H NMR, ¹³C NMR, dynamic light scattering (DLS) and scanning electron microscopy (SEM) methods. All the required solutions were prepared with a produced distilled water (electrical conductivity < 7.0 × 10⁻² μS cm⁻¹).

The analysis results are illustrated in the Supplementary information as Figs. S1 to S4, and the determined particle sizes with different criteria are summarized in Table 1. The purity of GSAIL was confirmed by appearing only the peaks of the GSAIL product in the ¹³CNMR and ¹HNMR spectra and none for the reactants and/or side products. The crude oil in this study was from an oil field in the

Table 1
The determined GSAIL sizes with different analysis methods.

SEM (nm)	Hydrodynamic DLS size (nm)	Micelle DLS size (nm)
11.9---27.5	0.7---5.0	200---580

Table 2
Major specifications of the used crude oil.

Spification/Composition	Value
°API	20.7
Saturated (wt%)	54.0
Aromatic (wt%)	22.3
Resin (wt%)	6.7
Asphalt (wt%)	7.7
Acidity number (mg KOH g ⁻¹)	0.09
Sulphur content (wt%)	1.63
Salt content (lbs per 1000 bbls)	4
Water content (wt%)	Nil
Density at 20 °C (g cm ⁻³)	0.915
Viscosity at 70 °F (cP)	55
Viscosity at 100 °F (cP)	44
Kinematic viscosity at 70 °F (cSt)	60
Pour point (°F)	10
Flashpoint (°F)	70
Reid vapor pressure (psi)	12.1
Loss at 200 °C (wt%)	9.3

southern Iran, for which the composition and the characteristics are listed in Table 2.

2.2. The main instruments and procedures

For measuring the IFT and contact angle values, a pendant drop tensiometer (manufacturer: Fars EOR Technology, model: CA-ES10) equipped with a digital monitoring system was used. Measurements were conducted by forming crude oil drops at the tip of a suitable size stainless steel needle, immersed in the continuous water phase. The setup and the method have been widely described in our previous reports (Kharazi et al., 2019, Saïen et al., 2019). The IFT (γ) was determined by analyzing the shape of formed drops in relation to the force balance of buoyancy and of interfacial tension established with an automatic image processing system based on the following equation (Stauffer, 1965):

$$\gamma = \frac{\Delta\rho g D^2}{H} \quad (1)$$

In this equation, $\Delta\rho$ represents difference between the crude oil and aqueous solution densities, g is the gravitational acceleration constant, D is the forming drop equatorial diameter, and finally, H is the drop shape parameter whose correlation and the involved parameters have been precisely reported in the literature (Drelich et al., 2002).

Using this method, an IFT of 31.8 mN·m⁻¹ was measured for pure crude oil–water system at 298.2 K. To ensure the accuracy, the IFT of pure water–air system (as surface tension) was also mea-

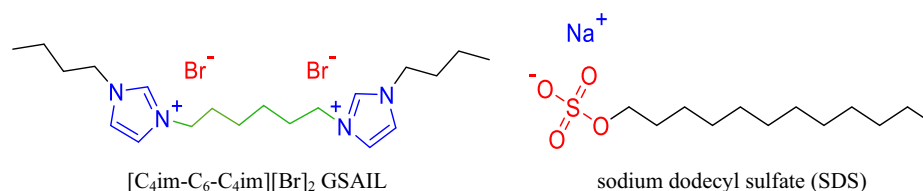


Fig. 1. Chemical structures of [C₄im-C₆-C₄im][Br]₂ (a) and sodium dodecyl sulfate (SDS) (b) surfactants.

sured at 298.2 K as 71.9 mN·m⁻¹, very close to 72.0 mN·m⁻¹ in the literature (Lan et al., 2016). All measurements (at least twice) were carried out under ambient pressure and at the temperatures of 298.2 K that was adjusted by means of a thermostat (0.1 K uncertainty).

The concentration ranges of the individual GSAIL, SDS solutions as well as their mixture were within (1.0 × 10⁻⁴ – 1.25) mol·dm⁻³ and (1.0 × 10⁻⁴ – 0.25) mol·dm⁻³, respectively. To this end, surfactants were weighed by means of a digital balance (uncertainty of 1.0 × 10⁻⁴ g). The mixing ratio of two substances was determined based on the mole fraction of GSAIL, $\alpha_1 = C_1/C_{12}$, in which C₁ and C₂, are respectively, the concentration of GSAIL and SDS, and also, C₁₂ = C₁ + C₂ stands for the concentration of the mixture. Perfect mole fraction range of $\alpha_1 = 0, 0.2, 0.3, 0.4, 0.5, 0.6, 0.8, \text{ and } 1$ were considered. The density of all the solutions was obtained using a U-tube oscillating densitometer (Anton Paar, DMA 4500, uncertainty 1.0 × 10⁻⁴ g·cm⁻³), with automatic viscosity correction. The CMCs were determined from the intersection of the upper and lower tangent lines of the breakpoint region in IFT variations versus surfactants concentration.

To evaluate emulsion formation, 2 cm³ of either of phases with a specific mole fraction and the typical concentration of 0.05 mol·dm⁻³ (corresponding to an intermediate IFT) were transferred to a glass vial. Each sample was then sonicated in a 40 kHz, 305 W ultrasound bath (SONICA 2400ETH S3) for 30 min. After resting for one day and one week, at 298.2 K, the resultant emulsion index was determined from the volumes of the formed emulsion (V_e) and the total sample volume (V_t) as V_e/V_t × 100 (Amani, 2015).

To measure the contact angles, a quartz plate was first immersed in the crude oil overnight (14 to 18 h) for aging and to be approximate to the real reservoir conditions. Subsequently, the crude oil was injected via a needle into the aqueous phase to release a drop to adhering to the top quartz plate (Saïen et al., 2015). After at least one hour, the image of the drop was recorded. The contact angles were then determined by analyzing of the hemisphere crude oil drop surrounded by different mole fraction solutions of the mixture of surfactants having a typical concentration of 0.05 mol·dm⁻³. An average contact angle for the left and the right sides of the hemispheres was automatically determined. All the measurements were performed at least twice to establish consistent results.

3. Results and discussion

3.1. IFT variations

3.1.1. Individual surfactants

The variation of the system IFT against the corresponding concentration are presented in Fig. 2. Evidently, either of the surfactants, brings about drastic decrease in the IFT up to CMC, from an initial value of 31.8 to 8.79 and 1.55 mN·m⁻¹ respectively. Under this condition, the intermolecular forces at the interface will diminish, leading to a large IFT reduction. Upon reaching CMC for GSAIL and SDS (0.68 and 0.06 mol·dm⁻³), the adsorbed particles completely saturate the interface with no free sites; thus, forcing the particles to self-assemble spontaneously. The corresponding obtained parameters are listed in Table 3. Comparison between the GSAIL and SDS in IFT reduction as well as the micelle formation, reveals that the longer alkyl chain SDS with 12 carbon chain outperforms the short chain GSAIL with 4 carbon atoms.

3.1.2. Theoretical consideration of individual surfactants

The Frumkin adsorption isotherm, which considers the non-ideal interactions (attraction or repulsion) among adsorbed particles at the interface, acceptably covers the IFT data with individual

surfactants (Birdi, 2009). Considering the two positively charged imidazolium rings in the [C₄im-C₆-C₄im][Br]₂ structure as well as anionic head group in SDS, giving strong interactions, the use of this isotherm is consistent. The equation of state and the isotherm are described as (Stubenrauch et al., 2005):

$$\Pi = -2RT\Gamma_{m,F}[\ln(1 - \theta) + \beta\theta^2] \quad (2)$$

$$b_F f_{\pm} [C(C + C_{\text{electrolyte}})]^{1/2} = \frac{\theta}{1 - \theta} \exp(-n\beta\theta) \quad (3)$$

Here, $\Pi = \gamma_0 - \gamma$ is known as interfacial pressure which represents difference between the pure system IFT, γ_0 , and the achieved value, γ . Besides, $\theta = \Gamma/\Gamma_{m,F}$ shows the interface coverage. Other parameters are the maximum interface excess concentration, $\Gamma_{m,F}$, the Frumkin adsorption constant, b_F , the van der Waals molecular interaction parameter, β , the activity coefficient of ions, f_{\pm} , and the number of cations and anions of the ionic surface-active substance, n . The correctness of fittings was established upon achieving a low value of the objective function (OF), which is described in details in our previous studies (Kharazi et al., 2019, Saïen et al., 2019). The achieved fitting parameters and the objective function, OF, are listed in Table 4.

As presented in Figs. S5 and S6, the adsorption isotherm of Frumkin fits the data very well. The low OF values confirm good fittings. The $\Gamma_{m,F}$ of the SDS with smaller volume and longer chain of 12 carbon atoms is higher than bulkier GSAIL with shorter chains of 4 carbon atoms, which is consistent with the above results relevant to greater hydrophobicity and more adsorption at the interface for longer hydrocarbons. Further, the negative value of the molecular interaction parameter, β , confirm the existence of electrostatic repulsion among GSAIL and SDS molecules. However, this parameter is higher for GSAIL because it has two positively charged rings per molecule, creating more electrostatic repulsion. In the same manner, the Frumkin adsorption constant, b_F , is obviously higher for SDS, which is due to greater hydrophobicity leading to higher adsorption tendency. Relevantly, the minimum occupied interface area by each adsorbed molecule, A_m , can be obtained from $A_m = 1/\Gamma_{m,F}N_{Av}$, where N_{Av} displays the Avogadro's number. As is expected, the compact orientation of SDS at the interface decreases the occupied area by each molecule, A_m , compared to GSAIL.

Meanwhile, the thermodynamic parameters of $\Delta G_{\text{ads}}^{\circ}$ and $\Delta G_{\text{mic}}^{\circ}$, related to adsorption and micellization Gibbs free energies, reflecting the adsorption and aggregation tendencies, can be determined as (Liu et al., 2012, Möbius et al., 2001):

$$\Delta G_{\text{ads}}^{\circ} = -2RT \ln\left(\frac{b_F \rho'}{2}\right) \quad (4)$$

$$\Delta G_{\text{mic}}^{\circ} = RT \ln \text{CMC} \quad (5)$$

while $\rho' = \rho/18$ is the molar concentration of water. As listed in Table 5, negative values of Gibbs free energies approve the GSAIL and SDS adsorption at crude oil–water interface and that the micellization was spontaneous. However, superior hydrophobicity with less electrostatic repulsion provides greater forces for SDS. As another point, for the both used surfactants, the absolute values of $\Delta G_{\text{ads}}^{\circ}$ are meaningfully greater than $\Delta G_{\text{mic}}^{\circ}$, implying that the surfactants prefer to adsorb instead of stay in the bulk to create aggregates.

3.1.3. Mixture of surfactants

The variation of the system IFT against the concentration of the surfactants mixture, at different GSAIL mole fractions (α_1), are presented in Fig. 3. It can be seen that IFT decreases with concentration for all the mole fractions. Reasonably, easier interfacial

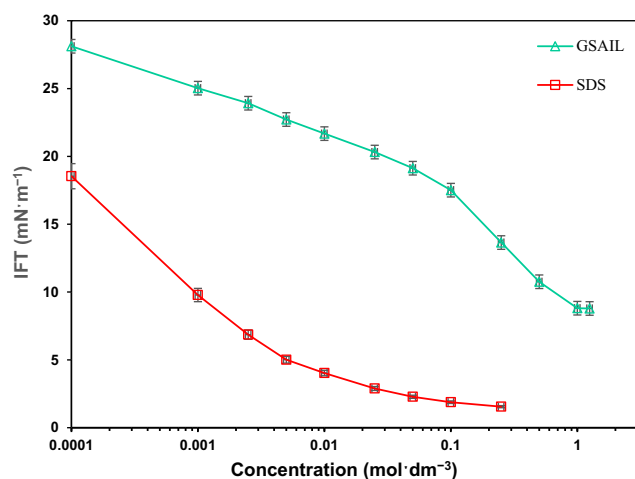


Fig. 2. The crude oil–water IFT variations with individual GSAIL and SDS concentration.

adsorption at low concentrations gives a steeper slope in IFT variation (Kharazi and Saïen, 2022b).

In another view, IFT changes versus α_1 , at different concentrations, are illustrated in Fig. 4. It can be seen that IFT significantly decreases with α_1 and then increases toward the IFT of just the GSAIL. The lowest IFT with the highest synergy is corresponding to the GSAIL mole fraction of about 0.4. If there was no synergy, the performance of the mixture was expected to lie along the straight lines between the IFTs of the individual components. To better clarify, the color synergistic regions are distinguished in Fig. 4.

To justify the synergy, the Rosen concept of dilution effect at the interface adsorption layer was employed (Rosen and Kunjappu, 2012). The level of synergism can be calculated as the percentage of difference between the achieved IFT and the linear contribution of the individual surfactant IFTs to the achieved IFT. Accordingly, a maximum 97.1 % synergism was relevant with 0.25 mol·dm⁻³ mixture of surfactants at $\alpha_1 = 0.4$, providing a low IFT value of 0.18 mN·m⁻¹. A low IFT is essential to have stable emulsions, required for efficient EOR processes, as it raises the capillary number in the reservoirs (Pillai et al., 2018, Zhang et al., 2009). From an economic point of view, use of low doses of surfactants is important to attain low IFT values. Another remarkable economy advantage is that experiments showed several times reusing of solutions with no sensible change in results.

In the same manner, the CMC reached to the very low value of 0.03 mol·dm⁻³ (89.6 % decrease compared to the linear contribution of individual surfactants) at $\alpha_1 = 0.4$. It is worth noting that the decrease in CMC is desired for EOR since it favors the transport

Table 3
CMC, IFT at CMC (γ_{CMC}), minimum reached IFT (γ_{min}) and maximum IFT reductions for individual surfactants.

Surfactant	CMC (mol·dm ⁻³)	γ_{CMC} (mN·m ⁻¹)	γ_{min} (mN·m ⁻¹)	Maximum IFT reduction (%)
GSAIL	0.68	9.9	8.8	72.4
SDS	0.06	2.1	1.5	95.1

Table 4

The maximum interface excess concentration, Γ_{mF} , the Frumkin adsorption constant, b_{F} , the interaction parameter, β , the minimum occupied interface area by each molecule, A_{m} , and the objective function, OF, for individual surfactants.

Surfactant	$\Gamma_{\text{mF}} \times 10^6$ (mol·m ⁻²)	b_{F} (dm ³ ·mol ⁻¹)	β	$A_{\text{m}} \times 10^{36}$ (m ²)	OF
GSAIL	0.77	1.53×10^2	-6.2	15.13	0.116
SDS	0.91	5.67×10^3	-3.6	12.80	0.335

Table 5

Gibbs free energy of adsorption, $\Delta G_{\text{ads}}^{\circ}$, Gibbs free energy of micellization, $\Delta G_{\text{mic}}^{\circ}$, and the molar concentration of water, ρ' , for individual surfactants.

Surfactant	$\Delta G_{\text{ads}}^{\circ}$ (kJ·mol ⁻¹)	$\Delta G_{\text{mic}}^{\circ}$ (kJ·mol ⁻¹)	$\rho' \times 10^3$ (mol·cm ⁻³)
GSAIL	-75.62	-0.96	55.38
SDS	-93.51	-6.97	54.38

of oil droplets with micelles in the surfactant flooding process (Saïen et al., 2022).

With respect to the chemical structure of surfactants (Fig. 1), due to the attraction between two positively charged imidazolium rings of the GSAIL and the negatively charged hydrophilic SDS head group, a close orientation at the interface would be established bringing about high IFT reductions. A similar mechanism can be interpreted for the micelle formation. Fig. 5 schematically presents the arrangement of the surfactant molecules in the bulk and at the interface. Considering two positively charged rings in the GSAIL and one negative charge in SDS molecules, the highest dilution effect as well as the maximum degree of synergy was found at the ratio of 4:6 for GSAIL:SDS i.e. $\alpha_1 = 0.4$. At higher mole fractions, the percentage of synergy decreases due to disrupting the balance between electrostatic interactions. Based on the results, it can be concluded that the adsorbed layers are different for different bulk mole fractions (Saïen and Asadabadi, 2011).

For a better comparison, variation of the maximum percentage of synergism (at $\alpha_1 = 0.4$), with the concentration of the mixtures is shown in Fig. 6. As can be seen, maximum percentage of synergism rises incredibly at low concentrations, tends to low variations after 0.01 mol·dm⁻³ and remains almost constant, around 97 %, for concentrations more than 0.10 mol·dm⁻³. At low concentrations, due to provided space, positive and negative charged molecules are better placed next to each other, significantly neutralize the electrostatic repulsion and thus, synergism rises. However, at high concentrations, the closer orientation of the adsorbed molecules gives greater electrostatic repulsion.

3.1.4. Theoretical investigation for the mixture of surfactants

The Rosen non-ideal interactions in binary mixtures (NIBM) theory (Rosen and Kunjappu, 2012), was used to determine the mole fraction of adsorbed compounds (X_1 for the GSAIL as surfactant 1) and the parameter of molecular interaction between adsorbed components (β) using the following equations (Rosen and Kunjappu, 2012):

$$\frac{(X_1)^2 \ln(C_{12}\alpha_1/C_1^0 X_1)}{(1-X_1)^2 \ln[C_{12}(1-\alpha_1)/C_2^0(1-X_1)]} = 1 \quad (6)$$

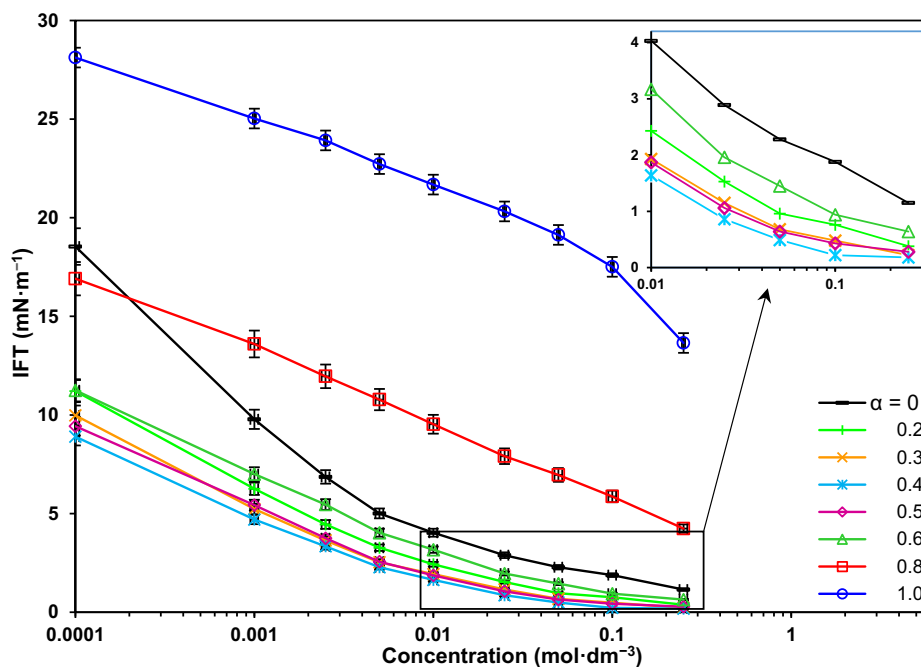


Fig. 3. The IFT variations with the concentration of the mixture of surfactants.

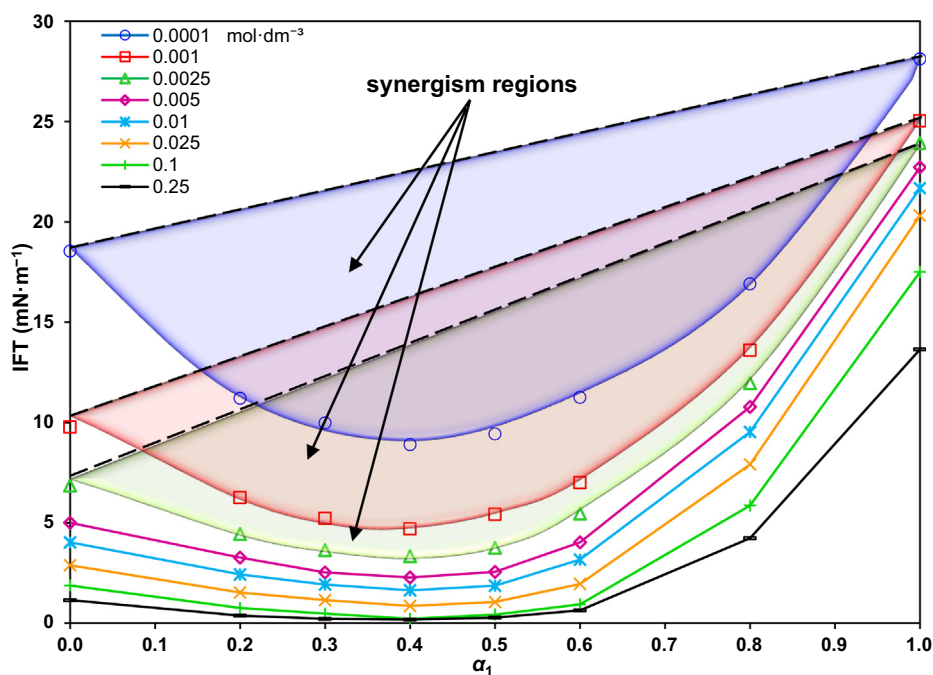


Fig. 4. Synergism regions for different mole fraction of the GSAIL and concentration of the mixture.

$$\beta = \frac{\ln(C_{12}\alpha_1/C_1^0X_1)}{(1 - X_1)^2} \quad (7)$$

while α_1 is the mole fraction of surfactant 1 (GSAIL) in the bulk solution and C_1^0, C_2^0 , and C_{12} are respectively, the bulk concentration of surfactant 1 (GSAIL), surfactant 2 (SDS), and their mixture. The C_1^0, C_2^0 and C_{12} values for a specified IFT, were determined from the graphs of IFT against the concentration of individual and the

mixture of surfactants at a certain α_1 (Fig. S7). The corresponding values are listed in Table S1. After that, the exact values of X_1 and β were calculated from above equations by iteration method (Saïen and Asadabadi, 2011). Based on NIBM theory, the negative β values roughly indicate attractive interactions and positive values repulsive interactions at the interface. The determined values of the parameters at selected IFTs of 1, 2.5, 5, 10 and 15 $\text{mN}\cdot\text{m}^{-1}$ are presented in Table 6. As illustrated in Fig. 7, the maximum X_1

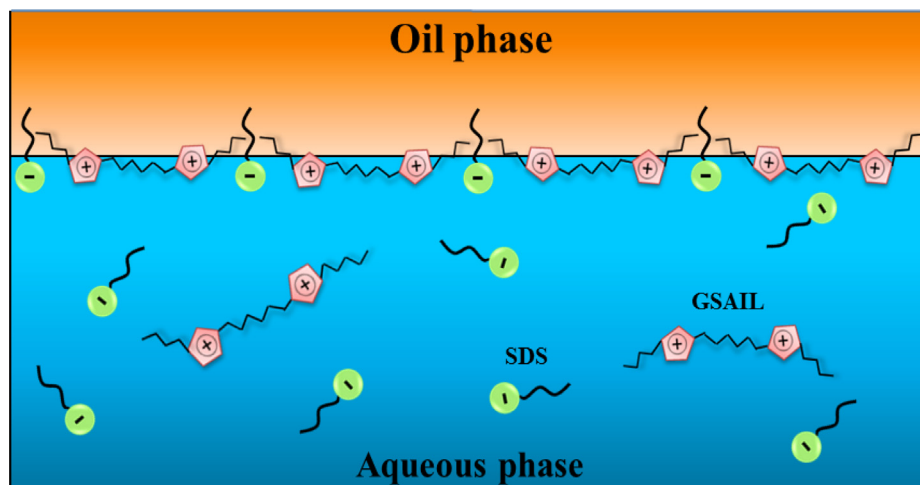


Fig. 5. Schematic arrangement of the GSAIL and SDS molecules in the crude oil–water system.

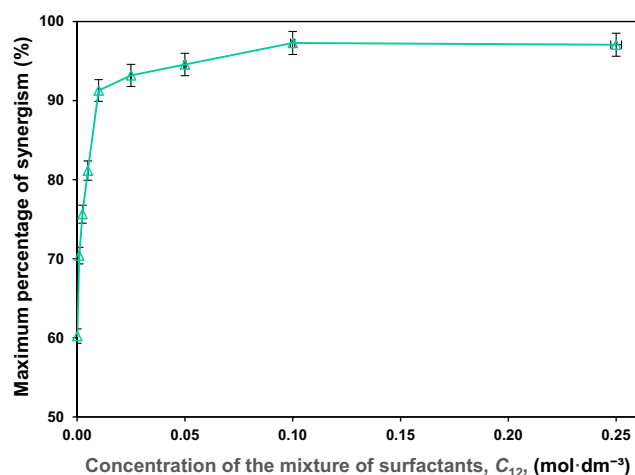


Fig. 6. Maximum percentage of synergism, at $\alpha_1 = 0.4$, versus concentration of the mixture of surfactants.

is achieved at $\alpha_1 = 0.4$, corresponding to the highest degree of synergism. These results confirm that the dilution effect causes more interfacial adsorption of the surfactants, which is the main reason of synergy.

The interfacial molecular interaction parameter, β , variation versus α_1 is shown in Fig. 8. Negative β values indicate that the surfactants exhibit attractive interaction despite the dominant self-repulsive interaction between just either of surfactants. Therefore, the larger absolute value of β , the stronger synergistic effect would be (Olea and Gamboa, 2003). It can also be seen that the highest absolute interaction between the compounds corresponds to $\alpha_1 = 0.4$, consistent with the above results.

3.2. Emulsifying capability

Transferring surfactants to the low permeable zones and dissolving crude oil via stable oil-in-water (O/W) is vital in EOR. Noteworthy, the formation of emulsions reduces the adsorption of crude oil on the surface of the reservoir rocks and smoothen the movement of the residual crude oils (Guang et al., 2018). Besides, emulsions facilitate the flow of injection fluids in non-swept areas, blocks permeable pathways to inhibit the crude oil

Table 6

The interfacial mole fraction (X_1) and the interfacial molecular interaction parameter (β) for different bulk mole fraction of the GSAIL (α_1) and selected IFTs.

α_1	IFT ($\text{mN}\cdot\text{m}^{-1}$)	X_1	β
0.2	1.0	0.21	-7.57
	2.5	0.24	-11.61
	5.0	0.27	-13.37
	10.0	0.31	-16.32
	15.0	0.35	-16.41
0.3	1.0	0.24	-8.52
	2.5	0.27	-12.85
	5.0	0.30	-15.30
	10.0	0.33	-19.39
	15.0	0.36	-24.58
0.4	1.0	0.29	-9.42
	2.5	0.35	-13.55
	5.0	0.36	-19.12
	10.0	0.37	-23.55
	15.0	0.38	-28.18
0.5	1.0	0.28	-9.10
	2.5	0.31	-12.68
	5.0	0.33	-14.53
	10.0	0.36	-20.92
	15.0	0.37	-31.05
0.6	1.0	0.26	-9.06
	2.5	0.29	-12.68
	5.0	0.31	-12.37
	10.0	0.35	-17.40
	15.0	0.36	-22.58

backflow, raises the viscosity of the displacement medium, and greatly improves the mobility as well as the sweeping efficiency (Yazhou et al., 2017, Mandal et al., 2010). Hence, a low IFT is essential for stable emulsions.

The images of the produced emulsions with different mole fraction of mixtures at typical concentration of $0.05 \text{ mol}\cdot\text{dm}^{-3}$ (corresponding to an intermediate IFT) are presented in Fig. 9. As is clear, the emulsion is well formed in the presence of the surfactants. These confirm that the mixture of surfactants is a suitable candidate for EOR.

For a better comparison, the emulsion indices for different mole fractions after one day and one week are shown in Fig. 10. As expected, the maximum emulsification indices correspond to the highest synergistic degree at $\alpha_1 = 0.4$, bringing about emulsion indices as high as 75.1 and 69.8 % after one day and after one week, giving 44.8 and 52.0 % synergism, respectively. The emulsions were also monitored after two months and, interestingly, their stability

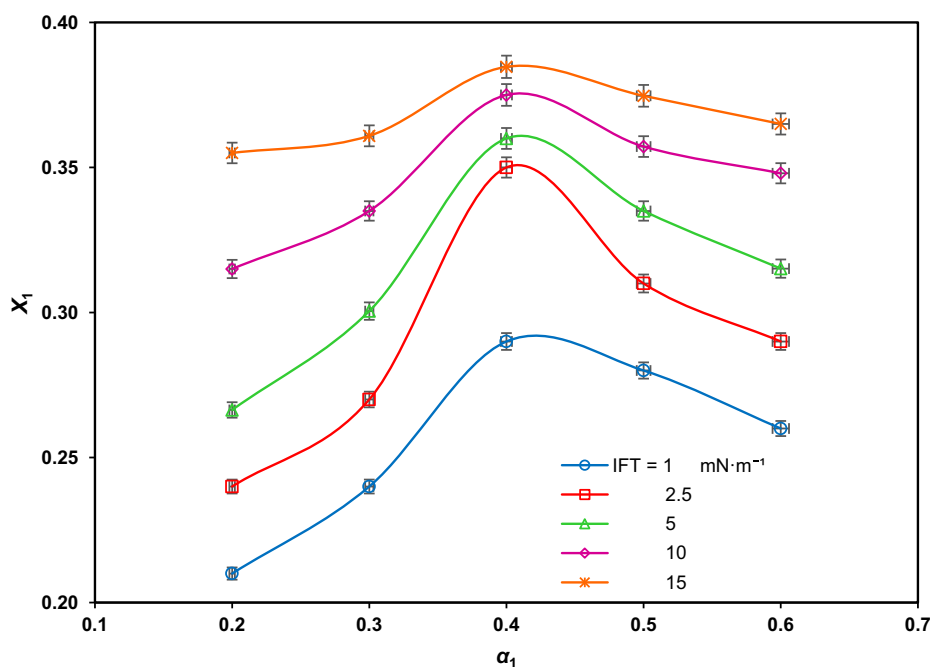


Fig. 7. The mole fraction of GSAIL at the interface versus its bulk mole fraction for different IFTs.

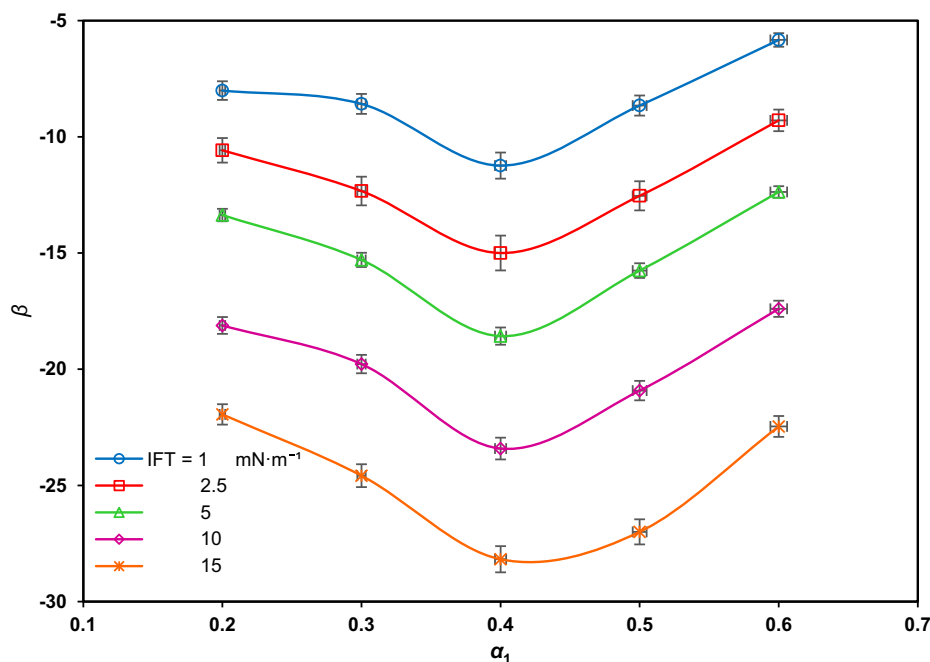


Fig. 8. The interfacial molecular interaction parameter versus the GSAIL bulk mole fraction for different IFTs.

was proved as there was no sensible change in the emulsions. This is a consequence of more directional adsorption of surfactants around the interface of crude oil droplets and the formation of hydrophilic protective films, playing a prominent role in the dispersion of phases (Gao and Sharma, 2013). Noteworthy, creating stable emulsions with individual surfactants regularly requires co-surfactants which are volatile and present environmental hazards (Saien et al., 2022); however, it is beneficial here that the mixture of surfactants form stable emulsions with no aid of a harmful

co-surfactant (Bera and Belhaj, 2016, Rodríguez-Escontrela et al., 2016).

3.3. Wettability alteration

Known as a critical factor, wettability represents the interaction between the rock surface of the reservoir in contact with crude oil and aqueous solutions affecting the residual original oil in place (OOIP). As the wettability changes from oil-wet to water-wet, the

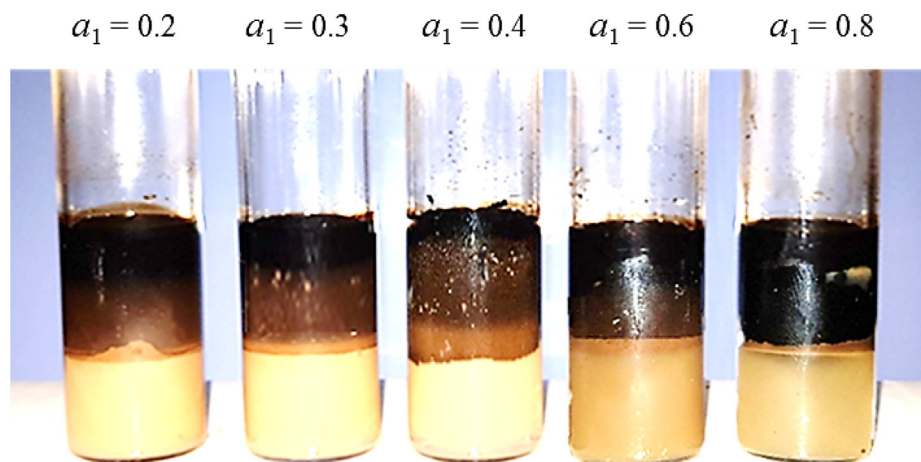


Fig. 9. Emulsions with 0.05 mol dm^{-3} of the surfactants mixture under different GSAIL bulk mole fractions after one day.

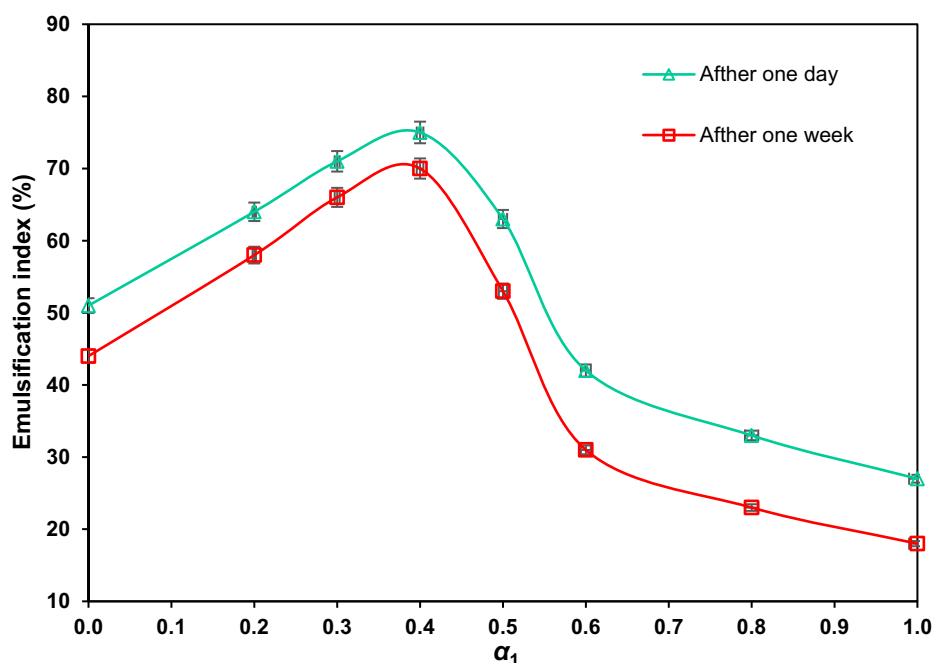


Fig. 10. The emulsification index versus GSAIL mole fraction with 0.05 mol dm^{-3} of the surfactants mixture after one day and one week.

residual oil will detach easily from the surface of the reservoir rocks. This improves the mobility of the crude oil leading to a better EOR. In a crude oil–water–rock contact, reservoirs are considered as hydrophilic (water-wet) with the contact angles within ($0 - 80^\circ$), moderate (intermediate-wet) within ($80 - 100^\circ$) and hydrophobic (oil-wet) within ($100 - 180^\circ$) (He et al., 2015).

The appeared shapes of the attached drops, surrounded by different mole fractions of the mixture of surfactants under typical 0.05 mol dm^{-3} concentration, the measured contact angles and the corresponding wettability state, are precisely given in Table 7 and presented in Fig. 11. The reason for choosing the mentioned concentration is the high level revealed synergy (Fig. 6), and allowing correct comparison (Kharazi and Saien, 2023, Saien et al., 2023). As it is possible to see, the contact angles of 130° and 100° with, respectively, just GSAIL and SDS, are drastically reduced to 45° at $\alpha_1 = 0.4$ with the highest degree of synergism of 59.8 %.

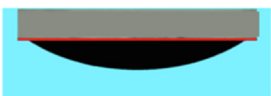
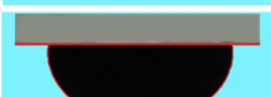
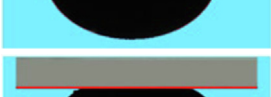
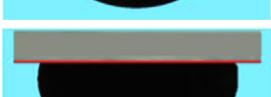
4. Conclusions

The effects of the mixture of $[\text{C}_4\text{im-C}_6\text{-C}_4\text{im}][\text{Br}]_2$ cationic nano GSAIL and the SDS anionic surfactant on curing interfacial properties of the crude oil–water system were studied. The individual surfactants could diminish the crude oil–water IFT. In theoretical study, the Frumkin adsorption model was able to reproduce the data with reasonable parameter values.

Thanks to their matched molecular interactions, the mixture of the surfactants reduced the IFT much stronger than just the linear contribution of individual surfactants and providing a low IFT value under the GSAIL mole fraction of 0.4. This synergism is a consequence of interactions between the cationic GSAIL and the anionic surfactant. In the same manner, CMC was highly reduced. The obtained results for the mixture of surfactants were analyzed by NIBM theory and the related parameters were determined.

Table 7

The shapes of the drops on the solid surface surrounded by different mole fractions of the mixture of surfactants, the contact angle and the wettability state at the typical concentration of 0.05 mol dm^{-3} .

Mole fraction	Image	Contact angle	State
Pure water		$\theta = 158^\circ$	oil-wet
$\alpha_1 = 0$		$\theta = 100^\circ$	intermediate-wet
$\alpha_1 = 0.2$		$\theta = 68^\circ$	water-wet
$\alpha_1 = 0.3$		$\theta = 53^\circ$	water-wet
$\alpha_1 = 0.4$		$\theta = 45^\circ$	water-wet
$\alpha_1 = 0.5$		$\theta = 77^\circ$	water-wet
$\alpha_1 = 0.6$		$\theta = 95^\circ$	intermediate-wet
$\alpha_1 = 0.8$		$\theta = 116^\circ$	oil-wet
$\alpha_1 = 1.0$		$\theta = 130^\circ$	oil-wet

The emulsification study revealed that the mixture of surfactants could create stable dispersion of crude oil in aqueous phase. Furthermore, the effect of mixture of surfactants on the wettability alteration showed transferring from oil-wet to water-wet because of reducing the adhesion of the crude oil to the solid surface.

The results totally demonstrated that the mixture of surfactants exhibit much better performance while using low concentrations. However, their performance at field should be sufficiently explored to find out the effects of operational parameters.

Declaration of Competing Interest

The authors declare that they have no known competing financial interests or personal relationships that could have appeared to influence the work reported in this paper.

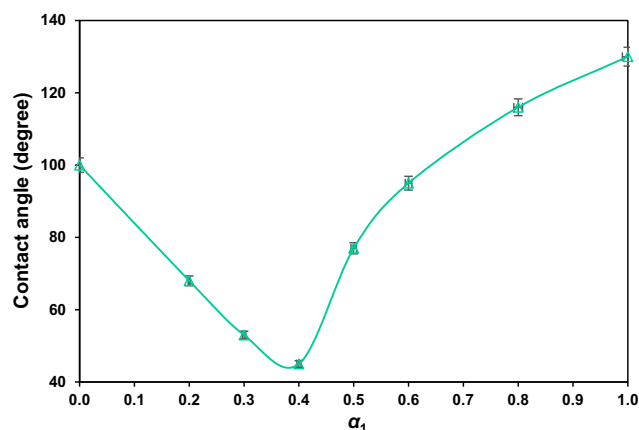


Fig. 11. The quartz-crude oil-aqueous phase contact angle versus GSAIL bulk mole fraction under surfactants mixture concentration of 0.05 mol dm^{-3} .

Acknowledgments

The authors would like to acknowledge the Bu-Ali Sina University for the financial support of this research.

References

- Amani, H., 2015. Evaluation of biosurfactants and surfactants for crude oil contaminated sand washing. *Pet. Sci. Technol.* 33, 510–519.
- Bera, A., Belhaj, H., 2016. Ionic liquids as alternatives of surfactants in enhanced oil recovery a state-of-the-art review. *J. Mol. Liq.* 224, 177–188.
- Birdi, K.S. *Surface and Colloid Chemistry: Principles and Applications* (CRC press) 2009.
- Chen, C., Wang, S., Kadhum, M.J., Harwell, J.H., Shiao, B.J., 2018. Using carbonaceous nanoparticles as surfactant carrier in enhanced oil recovery: A laboratory study. *Fuel* 222, 561–568.
- Drelich, J., Fang, C.H., White, C.L., 2002. Measurement of interfacial tension in fluid-fluid systems. *Ency. Surf. Colloid Sci.* 3, 3158–3163.
- Ezzat, A., Ayman, O., Atta, M., Al-Lohedan, H.A., 2021. Demulsification of stable seawater/Arabian heavy crude oil emulsions using star-like tricationic pyridinium ionic liquids. *Fuel* 304, 121436.
- Gao, B., Sharma, M.M., 2013. A family of alkyl sulfate gemini surfactants. 1. Characterization of surface properties. *J. Colloid Interface Sci.* 404, 80–84.
- Guang, Z.H., Caili, D.A., Qing, Y.O., 2018. Characteristics and displacement mechanisms of the dispersed particle gel soft heterogeneous compound flooding system. *Pet. Explor. Dev.* 45, 481–490.
- He, L., Lin, F., Li, X., Sui, H., Xu, Z., 2015. Interfacial sciences in unconventional petroleum production: from fundamentals to applications. *Chem. Soc. Rev.* 44, 5446–5494.
- Hou, J., Song, F., Ji, X., Lin, S., 2022. Ionic liquids enhanced oil recovery from oily sludge-experiment and mechanism. *Arab. J. Chem.* 15, 104210.
- Hui, K., Tang, J., Lu, H., Xi, B., Qu, C., Li, J., 2020. Status and prospect of oil recovery from oily sludge: A review. *Arab. J. Chem.* 13, 6523–6543.
- Jia, H., Leng, X., Hu, M., Song, Y., Wu, H., Lian, P., Liang, Y., Zhu, Y., Liu, J., Zhou, H., 2017. Systematic investigation of the effects of mixed cationic/anionic surfactants on the interfacial tension of a water/model oil system and their application to enhance crude oil recovery. *Colloids Surf. A Physicochem. Eng. Asp.* 529, 621–627.
- Kharazi, M., Saïen, J., Asadabadi, S., 2022. Review on amphiphilic ionic liquids as new surfactants: from fundamentals to applications. *Top. Curr. Chem.* 380, 1–44.
- Kharazi, M., Saïen, J., 2022a. Mechanism responsible altering in interfacial tension and emulsification of the crude oil-water system with nano Gemini surface active ionic liquids, salts and pH. *J. Pet. Sci. Eng.* 219, 111090.
- Kharazi, M., Saïen, J., 2022b. Upgrading the properties of the crude oil-water system for EOR with simultaneous effects of a homologous series of nanogemini surface-active ionic liquids, electrolytes, and pH. *ACS Omega* 7, 40042–40053.
- Kharazi, M., Saïen, J., Yarie, M., Zolfigol, M.A., 2019. Different spacer homologs of gemini imidazolium ionic liquid surfactants at the interface of crude oil-water. *J. Mol. Liq.* 296, 111748.
- Kharazi, M., Saïen, J., Yarie, M., Zolfigol, M.A., 2021. Promoting activity of gemini ionic liquids surfactant at the interface of crude oil-water. *Pet. Res.* 117, 113–123.
- Kharazi, M., Saïen, J., Torabi, M., Zolfigol, M.A., 2023. Green nano multicationic ionic liquid based surfactants for enhanced oil recovery: A comparative study on design and applications. *J. Mol. Liq.* 383, 122090.

- Lan, M., Wang, X., Chen, P., Zhao, X., 2016. Effects of surface tension and wood surface roughness on impact splash of a pure and multi-component water drop. *Case Stud. Therm. Eng.* 8, 218–225.
- Liu, G., Gu, D., Liu, H., Ding, W., Luan, H., Lou, Y., 2012. Thermodynamic properties of micellization of Sulfobetaine-type Zwitterionic Gemini Surfactants in aqueous solutions—A free energy perturbation study. *J. Colloid Interface Sci.* 375, 148–153.
- Mandal, A., Samanta, A., Bera, A., Ojha, K., 2010. Characterization of oil– water emulsion and its use in enhanced oil recovery. *Ind. Eng. Chem. Res.* 49, 12756–12761.
- Möbius, D., Miller, R., Fainerman, V.B. *Surfactants: Chemistry, Interfacial Properties, Applications* (Elsevier) 2001.
- Nessim, M., Zaky, M., Deyab, M., 2018. Three new gemini ionic liquids: synthesis, characterizations and anticorrosion applications. *J. Mol. Liq.* 266, 703–710.
- Olea, A., Gamboa, C., 2003. Synergism in mixtures of cationic surfactant and anionic copolymers. *J. Colloid Interface Sci.* 257, 321–326.
- Pillai, P., Kumar, A., Mandal, A., 2018. Mechanistic studies of enhanced oil recovery by imidazolium-based ionic liquids as novel surfactants. *J. Indus. Eng. Chem.* 63, 262–274.
- Rodríguez-Escontrela, I., Rodríguez-Palmeiro, I., Rodríguez, O., Arce, A., Soto, A., 2016. Characterization and phase behavior of the surfactant ionic liquid tributylmethylphosphonium dodecylsulfate for enhanced oil recovery. *Fluid Phase Equilib.* 417, 87–95.
- Rosen, M.J., Kunjappu, J.T. *Surfactants and interfacial phenomena*. John Wiley & Sons.
- Saien, J., Asadabadi, S., 2011. Synergistic adsorption of Triton X-100 and CTAB surfactants at the toluene+ water interface. *Fluid Phase Equilib.* 307, 16–23.
- Saien, J., Kharazi, M., Asadabadi, S., 2015. Adsorption behavior of short alkyl chain imidazolium ionic liquids at n-butyl acetate+water interface: experiments and modeling. *Iran. J. Chem. Eng.* 12, 59–74.
- Saien, J., Kharazi, M., Yarie, M., Zolfigol, M.A., 2019. Systematic investigation of a surfactant type nano gemini ionic liquid and simultaneous abnormal salt effects on crude oil/water interfacial tension. *Ind. Eng. Chem. Res.* 58, 3583–3594.
- Saien, J., Kharazi, M., Pino, V., Pacheco-Fernández, I., 2022. Trends offered by ionic liquid-based surfactants: Applications in stabilization, separation processes, and within the petroleum industry. *Sep. Purif. Rev.* 2012, 1–29.
- Saien, J., Kharazi, M., Shokri, B., Torabi, M., Zolfigol, M.A., 2023. A comparative study on the design and application of new nano benzimidazolium Gemini ionic liquids for curing interfacial properties of crude oil–water system. *RSC Adv.* 13, 15747–15761.
- Stauffer, C.E., 1965. The measurement of surface tension by the pendant drop technique. *J. Phys. Chem.* 69, 1933–1938.
- Stubenrauch, C., Fainerman, V.B., Aksenenko, E.V., Miller, R., 2005. Adsorption behavior and dilational rheology of the cationic alkyl trimethylammonium bromides at the water/air interface. *J. Phys. Chem. B* 109, 1505–1509.
- Tamayo-Mas, E., Mustapha, H., Dimitrakopoulos, R., 2016. Testing geological heterogeneity representations for enhanced oil recovery techniques. *J. Pet. Sci. Eng.* 146, 222–240.
- Xu, Y., Wang, T., Zhang, L., Tang, Y., Huang, W., Jia, H., 2023. Investigation on the effects of cationic surface active ionic liquid/anionic surfactant mixtures on the interfacial tension of water/crude oil system and their application in enhancing crude oil recovery. *J. Dispers. Sci. Technol.* 44, 214–224.
- Yazhou, Z., Demin, W., Zhipeng, W., Rui, C., 2017. The formation and viscoelasticity of pore-throat scale emulsion in porous media. *Pet. Explor. Dev.* 44, 111–118.
- Zhang, L., Geng, Y., Duan, W., Wang, D., Fu, M., Wang, X., 2009. Ionic liquid-based ultrasound-assisted extraction of fangchinoline and tetrandrine from *Stephania tetrandra*. *J. Sep. Sci.* 32, 3550–3554.